E-proceedings of the 38th IAHR World Congress
September 1-6, 2019, Panama City, Panama
doi:10.3850/38WC092019-0719

FREQUENCY AND TIME-DOMAIN ANALYSES OF PIPELINES ANCHORED AGAINST LONGITUDINAL MOVEMENT

DAVID FERRAS[(1)] & DIDIA COVAS[(2)]

[(1)] IHE-Delft Institute for Water Education, Delft, The Netherlands
d.ferras@un-ihe.org
[(2)] Instituto Superior Tecnico, Lisbon, Portugal
didia.covas@tecnico.ulisboa.pt

ABSTRACT

Frequency and time-domain approaches are used for the assessment of fluid-structure interaction during steady-oscillatory flows in straight pipe systems conditioned to anchor blocks. The first is developed based on the transfer matrix method (TMM), allowing the assessment of the system in terms of frequency response, while the second is based on the method of characteristics (MoC), allowing the assessment of wave propagation. Axial vibration of the fluid and the pipe-wall are solved and coupled by means of Poisson and junction coupling. The models are finally used to reproduce the performance of a marine outfall which steady-oscillatory flow is induced by the exposition to sea waves at the downstream pipe boundary. The complementarity of both approaches allows the co-verification of the models. Frequency-domain output enables the assessment of resonance frequencies for different pipe setups, while time-domain output allows a deeper insight of wave propagation.

Keywords: *Time-domain; frequency-domain; fluid-structure interaction; vibration modes; coupling; frequency response.*

NOTATION

A_f = fluid cross-sectional area (m^2)
a_f = pressure wave speed (ms^{-1})
A_s = pipe-wall cross-sectional area (m^2)
a_s = axial stress wave speed (ms^{-1})
D = pipe inner diameter (m)
E = pipe-wall Young's modulus (Pa)
e = pipe-wall thickness (m)
g = gravity acceleration (ms^{-2})
H = hydraulic head (m)
K = Bulk modulus of compressibility (Pa)
L = pipe length (m)
m_t = thrust block mass (kg)
p = fluid pressure (Pa)
Q = fluid discharge (m^3s^{-1})
r = inner radius of the pipe-wall (m)
t = time (s)
T_f = pressure wave period (s)
T_s = axial stress wave period (s)
U = pipe-wall velocity (ms^{-1})
V = fluid mean velocity (ms^{-1})
x = distance along the pipe axis (m)
f = specific weight of the fluid (kNm^{-3})
v = Poisson's ratio (-)
ρ_f = uid density (kgm^{-3})
ρ_s = pipe density (kgm^{-3})
σ = pipe axial stress (Pa)

1 INTRODUCTION

Fluid-structure interaction (FSI) and especially the behavior of pipe supports have a direct applicability in above-ground or non-buried pipe systems, such as hydropower systems, long oil and gas pipes, marine outfalls, cooling nuclear systems, thermal plants or any fluid distribution system in industrial compounds. However, only a few authors investigated anchor and support behavior in the context of water-hammer theory. Usually, studies are based on qualitative discussions focused on post-accident analyses and mitigation measures case-by-case oriented (Almeida & Koelle, 1992; Hamilton & Taylor,1996a,b; Locher et al., 2000).

The effect of pipe supports was considered from a time-domain perspective by Heinsbroek & Tijsseling (1994), who applied the method of characteristics for the fluid combined with a finite element method (FEM) for the structure. The study contributed to a better understanding of pipe supports rigidity and when these have to be taken into account in water-hammer analyses. The effect of pipe racks considering dry friction was assessed in Tijsseling & Vardy (1996), where recommendations to consider this effect were given. Following this line, Ferras et al. (2017, 2016a,b, 2018) carried out experimental and numerical work based on a straight copper pipe which allowed a broad variety of anchoring configurations.

In a frequency-domain framework additional insight is brought in terms of pipe vibration modes. In Zhang et al. (1999) a complete and comprehensive model development description for FSI problems in the frequency-domain by means of the Transfer Matrix Method (TMM) is provided; flexural and axial pipe vibrations were coupled with transient hydraulics and a set of benchmark problems were presented. Wu & Shih (2001) and Yang et al. (2004) used the TMM to simulate a multi-span pipe system with rigid constraints at the middle section, concluding that the effect of junction coupling was dominant versus Poisson coupling.

The present research work aims at providing further insight in the problem of fluid-structure interaction during steady-oscillatory flows considering the axial pipe vibration constrained by different anchoring conditions. Both frequency and time-domain approaches are used for the sake of problem description completeness. The models are first verified by means of benchmark problems and then applied to describe the performance of a marine outfall exposed to sea waves. To the knowledge of the authors, FSI analyses in frequency and time-domains considering steady-oscillatory flows have never been applied to marine outfalls.

2 NUMERICAL MODEL DEVELOPMENT

2.1 Governing equations

The models implemented hereby are based on a set of partial differential equations composed by Eqs. (1) to (4), where beam equations for the longitudinal vibration of thin cylindrical tubes (Weaver Jr et al., 1990) are combined with water-hammer equations for the pressure wave propagation in conduits (Chaudhry, 2014). For the sake of simplicity friction dissipation is neglected.

$$\frac{\partial V}{\partial t}+\frac{1}{\rho_f}\frac{\partial p}{\partial x}=0 \tag{1}$$

$$\frac{\partial V}{\partial x}+\frac{1}{\rho_f a_f^2}\frac{\partial p}{\partial t}=\frac{2\nu}{E}\frac{\partial \sigma}{\partial t} \tag{2}$$

$$\frac{\partial U}{\partial t}-\frac{1}{\rho_s}\frac{\partial \sigma}{\partial x}=0 \tag{3}$$

$$\frac{\partial U}{\partial x}-\frac{1}{\rho_s a_s^2}\frac{\partial \sigma}{\partial t}=-\frac{r\nu}{eE}\frac{\partial p}{\partial t} \tag{4}$$

2.2 Time-domain implementation

The time-domain numerical implementation is fully based on the one presented in Ferras (2016), which, at the same time, its fundamental numerical scheme was based on Tijsseling (1993). In these studies a MoC approach was used to simulate all the coupling mechanisms, hereby though friction is neglected so the focus is only on the Poisson and junction coupling mechanisms. The former is included in the governing equations (Eqs. 2 and 4), while the latter is defined in the pipe boundary conditions. Details of the model implementation can be found in Ferras (2016) and Ferras et al. (2017).

The code was successfully tested and verified by means of the benchmark problems presented in Tijsseling & Lavooij (1990) and Lavooij & Tijsseling (1989), for which Problem-A consists of a reservoir-pipe-valve system with pipe length L = 20 m, inner radius r = 398.5 mm, pipe-wall thickness e = 8 mm, Young's modulus E = 210 GPa, solid density ρ_s = 7900 kg/m3, Poisson ratio ν = 0.30, bulk modulus K = 2.1 GPa, fluid density ρ_f = 1000 kg/m3 and initial flow velocity V0 = 1 m/s. The valve is closed in one time-step, and both boundary conditions fixed and free moving valve are analyzed.

Figure 1 shows the output from such verifications.

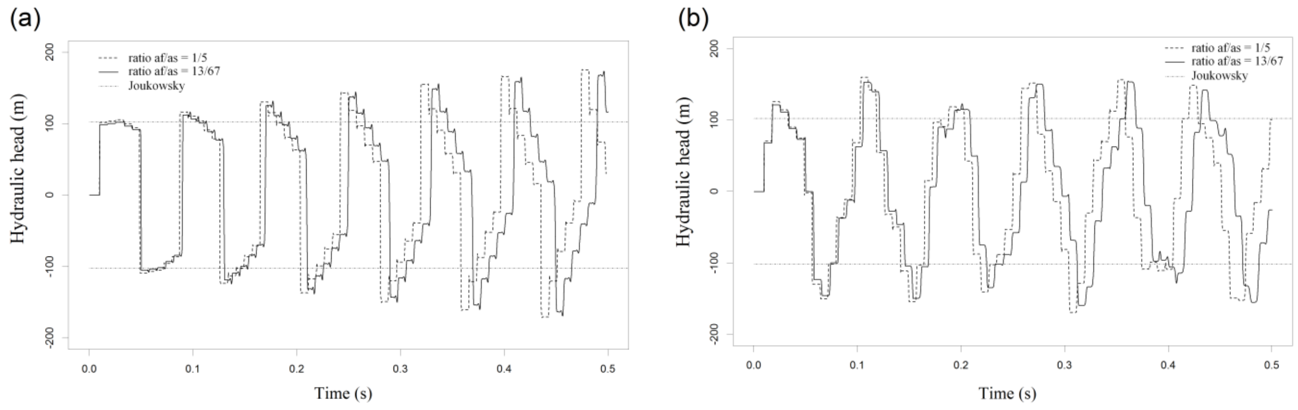

Figure 1. Delft Hydraulics benchmark Problem A with (a) fixed boundaries and (b) with a free moving valve.

2.3 Frequency-domain implementation

The frequency-domain code is based on the one proposed for axial pipe vibration in Zhang et al. (1999). TMM is, therefore, the method implemented and Poisson and junction coupling are considered. Like in the time-domain analysis Poisson coupling is nested in the governing equations, while junction coupling is defined at the boundaries. The excitation source inducing steady-oscillatory flow is located at the boundaries. Details of the model implementation can be found in Zhang et al. (1999).

The problem suggested in Zhang et al. (1999) (example B2) was replicated for the verification of the TMM implementation. The problem is based on the same pipe-reservoir-valve system described in section 2.2, which is again excited to a water-hammer event but now assessed from the perspective of frequency response.

Figure 2 shows the model output, which is successfully in agreement with the one presented in Zhang et al. (1999).

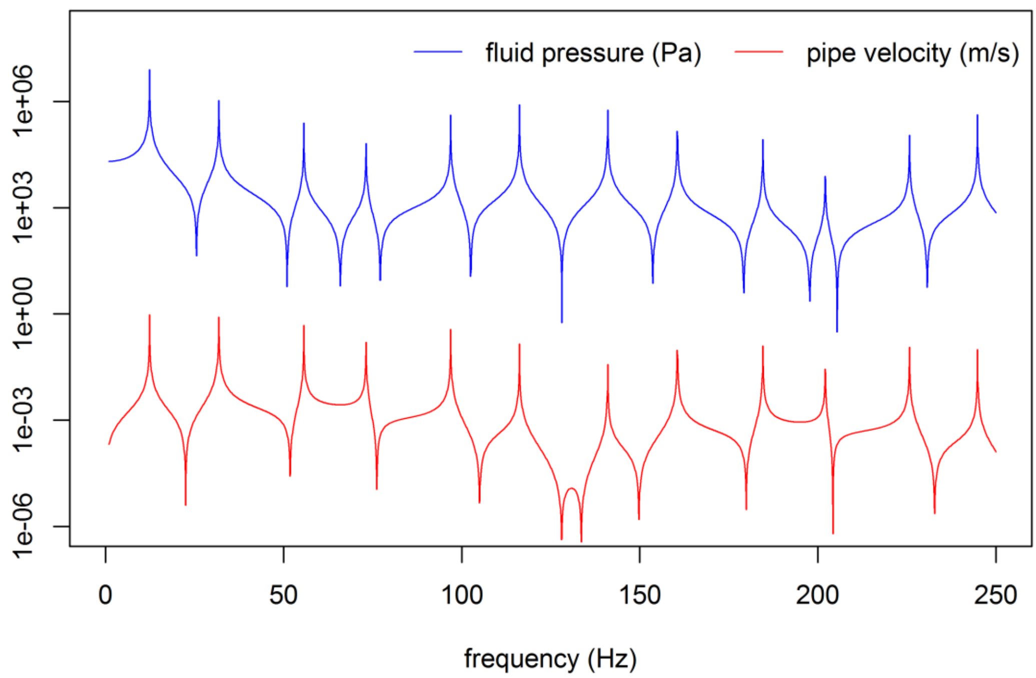

Figure 2. Pipe velocity and fluid pressure during water-hammer at unrestrained valve.

These benchmark problems established on numerical model results (Figs. 1 and 2) where respectively validated by means of experimental data in Tijsseling & Lavooij (1990) and Zhang et al. (1994), hence there is no need for further validation in the present study. As Figs. 1 and 2 correspond to the same pipe system, respective model verifications could have been presented in one single plot, either in the time-domain (*e.g.* applying inverse Fourier transform to frequency-domain output) or in the frequency-domain (*e.g.* applying Fourier transform to time-domain output). However, such co-verification (*vs.* validation) exercise can be carried out for any pipe configuration where the targeted pipe vibration modes are excited. Co-verification is shown therefore in the following section 3.1.

3 MODEL APPLICATION

3.1 Description of the pipe system

The conduit analyzed hereby is based on a marine outfall which was previously introduced in Larsen (1987), where the author described the development of steady-oscillatory flows in Danish sewage outfalls, which are normally disposed lying in shallow coasts and exposed to sea waves. Larsen (1987) highlighted the importance of considering resonant phenomena to ensure structural stability; the also author remarked the difficulty to assess such effects as normally measurements are only available at the upstream boundary.

The system analyzed can be schematized to a reservoir-pipe-reservoir system. The downstream reservoir though has an oscillating head according to sea wave conditions (*v.i.* Fig. 3). With a pipe length of L = 1200 m, a diameter of D = 0.5 m, and pipe wall thickness of e = 0.08 m, the pipe material is assumed to be HDPE and the respective water-hammer and axial stress wave celerities of a_f = 300 m/s and a_s = 900 m/s.

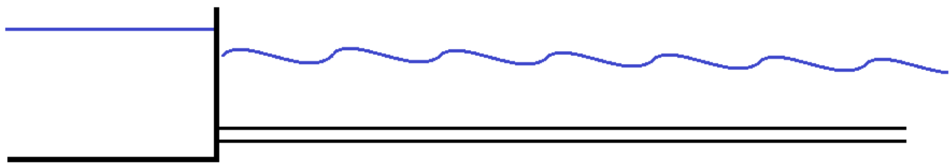

Figure 3. Schematic of the reservoir-pipe-reservoir system with the downstream reservoir representing sea conditions.

3.2 Model output

The pipe system presented in subsection 3.1 is tested for monochromatic pressure waves with varying period. The frequency response of the system is therefore assessed and resonance frequencies are characterized for three different setups:

- **Setup-1:** conduit anchored against longitudinal movement at the upstream and downstream pipe-ends.
- **Setup-2:** conduit anchored against longitudinal movement at the upstream pipe-end and free to move at the downstream pipe-end.
- **Setup-3:** conduit anchored against longitudinal movement at the upstream pipe-end and with a thrust block at the downstream pipe-end.

Table 1 summarizes the boundary conditions applied in each set-up.

Tab 1. Boundary conditions applied to the three assessed set-ups.

	Upstream Boundary	*Downstream Boundary*
Setup-1	$P = 0$ $U = 0$	$P = P_{sea}$ $U = 0$
Setup-2	$P = 0$ $U = 0$	$P = P_{sea}$ $U = 0$
Setup-3	$P = 0$ $U = 0$	$P = P_{sea}$ $A_s\sigma + s\, m_t\, U = 0$

Setups-1 and 2 are used to co-verify models by means of comparison between both approaches time and frequency domains (*v.i.* Figs. 4 and 5). Setup-3 is then used for a sensitivity analysis, testing first the effect of Poisson ratio for a free moving pipe-end and then the effect of a varying mass of a thrust block anchored at the downstream pipe-end (*v.i.* Figs. 6 and 7). Considering that the excitation source is located at the downstream pipe-end for all setups and that pressure is known at both ends (boundary conditions), the discussion of results focuses on the output concerning flow velocity and axial stress at the upstream pipe-end.

Setup-1: In this pipe configuration the conduit is constrained of movement at both ends but free to move in between. Hence, Poisson coupling occurs bringing the need of considering both solid and fluid axial vibrations. Figure 4 shows the frequency response of the pipe system based on both time and frequency domains approaches in terms of flow velocity at the upstream section. Good agreement between approaches is observed. The frequency response plot depicts not only the natural frequency and harmonics corresponding to the fluid vibration (water-hammer), but also of the axial pipe-wall vibration induced by the Poisson effect throughout the pipe. Considering the boundary conditions presented in Table 1, the water-hammer wave period is $T_f = 2L/a_f = 8$ s, while for the axial stress wave $T_s = 2L/a_s = 2.67$ s. Hence, the respective harmonics (in Hz) corresponding to the water-hammer wave are 0.125, 0.250, 0.375..., and for the axial stress are 0.375, 0.750, 1.125.... Consequently, as axial stress wave harmonics are a subset of those of water-hammer, only amplitude is modified in the frequency response diagram when FSI is considered in Setup-1.

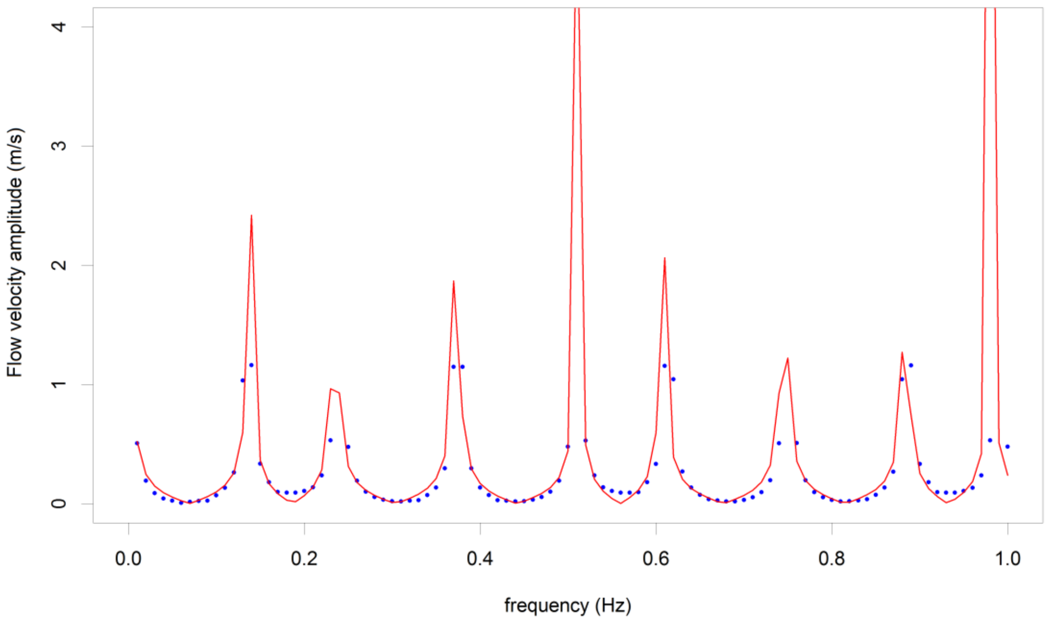

Figure 4. Frequency response considering anchored pipe-ends. Flow velocity output at the upstream section computed in the time-domain (blue dots) and in the frequency-domain (red line).

Setup-2: The pipe movement at the downstream end section is allowed, with an open end and no mass considered only Poisson coupling occurs. However, the new boundary condition modifies the axial stress wave period to $T_s = 4L/a_s = 5.33$ s. Hence, now the harmonics (in Hz) corresponding to this pipe vibration mode are: 0.1875, 0.375, 0.563, 0.750, 0.938... The new resonant frequencies corresponding to such harmonics can be clearly observed in the frequency response diagram depicted in Fig. 5. With consistency, both time and frequency-domain approaches are in agreement.

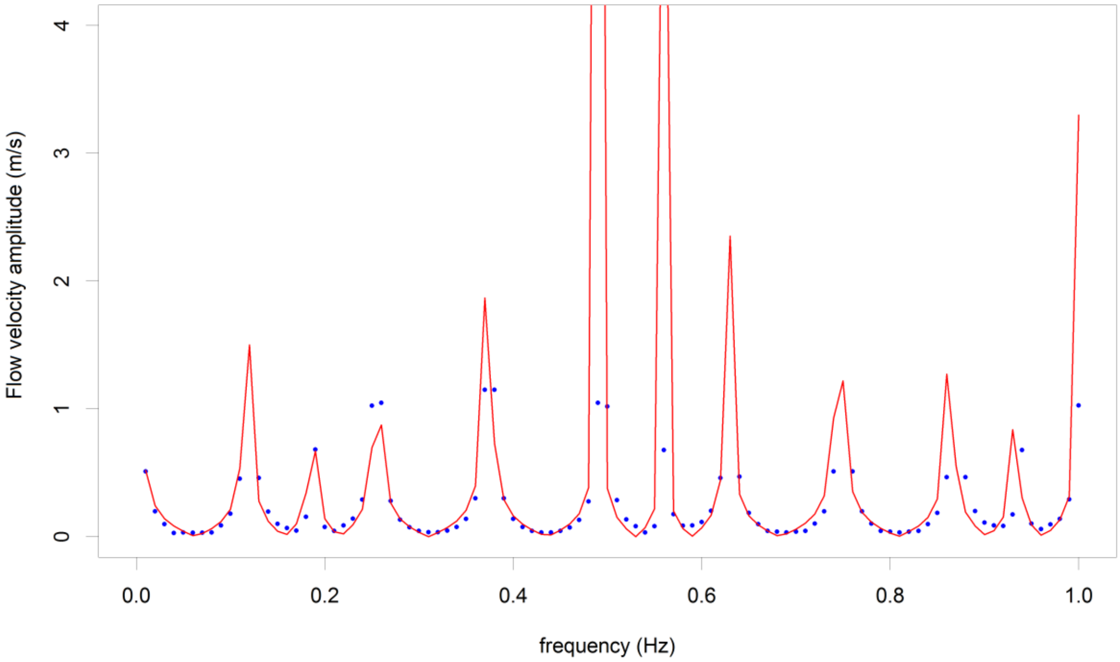

Figure 5. Frequency response considering non-anchored downstream end. Velocity output at the upstream section computed in the time-domain (blue dots) and in the frequency-domain (red line).

Setup-3: Resonance analyses are more efficient by means of direct computations in the frequency-domain (TMM) than by computations in the time-domain (MOC), which imply long and extensive series of simulations. As depicted in the previous paragraphs (Figs. 4 and 5) resonant frequencies (amplitude spikes) are clearly and exactly determined in the frequency-domain. Thus, the frequency-domain approach (TMM) is the one used to carry out a sensitivity analysis based on Setup-3, first focusing on the Poisson ratio parameter (Fig. 6) and, then, on the mass value of a downstream thrust block (Fig. 7). For the sake of clarity, dependent variables are plotted in a logarithmic scale.

Figure 6 shows the progress from a Poisson ratio $\nu = 0$ to $\nu = 0.5$. As there is no junction coupling, the first value of $\nu = 0$ is equivalent to the classic water-hammer model, where no FSI is considered. Then, as Poisson ratio values increase new harmonics corresponding to the axial stress wave emerge (*i.e.* 0.188 Hz, 0.375 Hz, 0.563 Hz, 0.750 Hz, 0.938 Hz...).

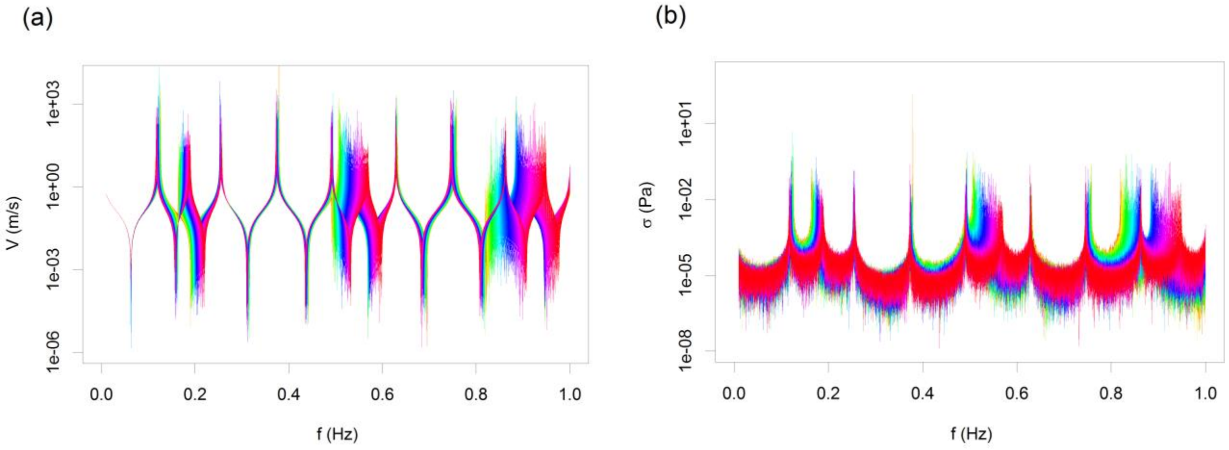

Figure 6. Frequency response considering a varying Poisson ratio from ν = 0 to ν = 0.5. Flow velocity amplitude (a) and axial stress amplitude (b) output at the upstream section. Warm colors for low Poisson ratio values and cold colors for high Poisson values.

Figure 7 shows the frequency response of the conduit progressing from a massless thrust block at the downstream end to a mass of m_t = 100 kg in intervals of 0.1 kg. Like in a pendulum, the natural frequencies of oscillation are independent of the thrust block mass. Hence, there are no new resonant frequencies in the fluid for the assessed solution domain (Fig. 7a), only some resonant amplitudes are affected. Concerning axial stress values (Fig. 7b), amplitudes experience a clear upward shift, while for some resonant frequencies apparently the amplitudes stay fixed. Somewhat, the upstream boundary seems to become a node for the harmonics corresponding to $Ts = 2L/a_s$.

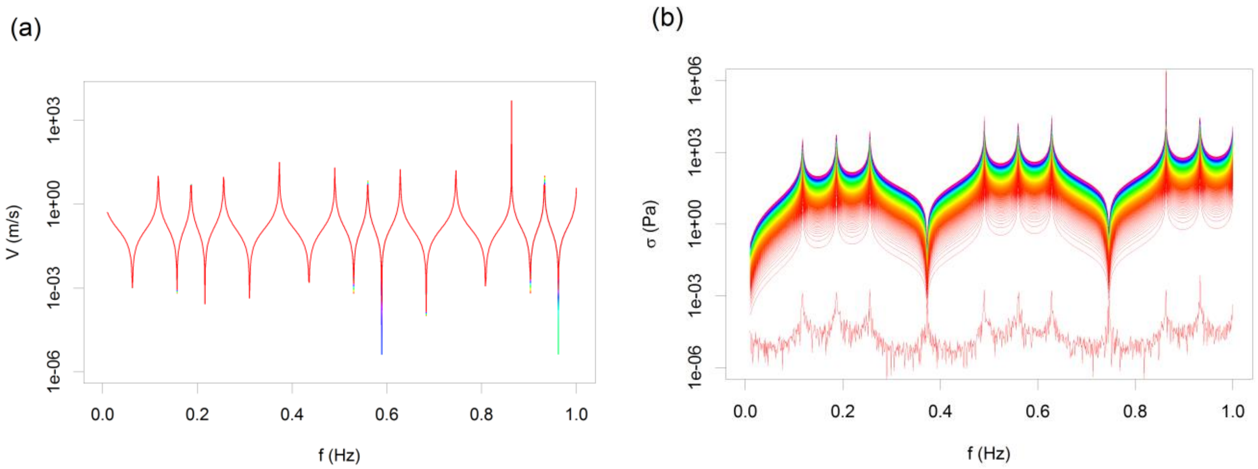

Figure 7. Frequency response for a varying thrust block mass from m_t = 0 to m_t = 100kg located at the downstream pipe-end. Flow velocity (a) and axial stress (b) output at the upstream section. Warm colors for low mass values and cold colors for high mass values.

Thinking in terms of wave propagation (*i.e.* time-domain) and how junction coupling is developed at the downstream section is helpful for the understanding of the frequency response amplitude shift depicted in Fig. 7b. In the Setup-3 junction coupling is not caused by an imbalance of direct pressure forces (as normally occurs) but only by the Poisson effect. In other words, the inner pressure causes a circumferential strain at the pipe wall which, due to Poisson effect, induces an axial strain. Because of this axial strain the thrust block is pushed/pulled axially and then the result of this action/reaction travels along the pipe to upstream. As shown in Setups-1 and 2 the axial stress wave harmonics corresponding to a pipe with anchored ends are a subset of the harmonics corresponding to a pipe with one only anchored end. Hence, for the complement of this subset of harmonics resonant frequencies are cancelled in the pipe-wall as consequence of the action/reaction (junction coupling) at the downstream section.

4 CONCLUSIONS

The presented research applies two fundamentally different approaches frequency and time-domains to solve a set of partial differential equations describing axial vibrations of the fluid and solid in closed conduits performing under steady-oscillatory flows. Respective models are successfully verified with benchmark problems and used to describe the performance of a marine outfall exposed to sea waves at its downstream boundary. As shown in the numerical output, this excitation source induces steady-oscillatory flow conditions which induce resonance for fluid and solid harmonics.

The consistency of the approaches is first confirmed by co-verification from a frequency domain perspective, hence transforming time-domain output to frequency response. At this stage two different pipe configurations (boundary conditions) are tested, Setup-1 with a fixed downstream boundary and Setup-2 with a downstream boundary free to move (massless and frictionless). In this comparison, different pipe harmonics corresponding to different pipe-wall axial vibration modes (natural frequencies) are observed.

A sensitivity analysis is carried out using Setup-3, which downstream boundary condition considers a thrust block adding inertia to the downstream section. The parameters analyzed are the Poisson ratio and the thrust block mass. The former allows the assessment of the transition from only one vibration mode (fluid) to two modes (fluid + solid), while the latter gives insight on the transition from a free moving to an anchored downstream boundary. The outcome of this sensitivity analysis suggests further investigation on those pipe harmonics corresponding to pipe-wall vibration modes.

ACKNOWLEDGEMENTS
The authors thank Dr. Arris S. Tijsseling (Eindhoven University of Technology, The Netherlands) for sharing with the authors very helpful notes used during the TMM implementation.

REFERENCES

Almeida, A. B. & Koelle, E. (1992). *Fluid transients in pipe networks*. Computational Mechanics Publ., Southampton, and Elsevier Applied Sci., London.

Chaudhry, M. H. (2014). *Applied Hydraulic Transients*, ISBN: 978-1-4614-8537-7. New York, NY: Springer.

Ferras, D. (2016). *Fluid-Structure Interaction during hydraulic transients in pressurized pipes: experimental and numerical analyses*. Ph.D. thesis, IST-EPFL No. 7099 and Communication 66, Laboratory of Hydraulic Constructions (LCH), Ed. A. Schleiss, Ecole Polytechnique Federale de Lausanne EPFL, Switzerland.

Ferras, D., Manso, P. A., Schleiss, A. J. & Covas, D. I. (2016a). Experimental distinction of damping mechanisms during hydraulic transients in pipe flow. *Journal of Fluids and Structures* 66, 424-446.

Ferras, D., Manso, P. A., Schleiss, A. J. & Covas, D. I. (2016b). Fluid-Structure Interaction in straight pipelines: Friction coupling mechanisms. *Computers & Structures* 175, 74-90.

Ferras, D., Manso, P. A., Schleiss, A. J. & Covas, D. I. (2017). Fluid-structure interaction in straight pipelines with different anchoring conditions. *Journal of Sound and Vibration* 394, 348{365.

Ferras, D., Manso, P. A., Schleiss, A. J. & Covas, D. I. (2018). Fluid-structure interaction in pipelines with anchor blocks against longitudinal movement. *Proc. of 13th Int Conf on Pressure Surges*, BHR Group, Bordeaux, France, 393-407.

Hamilton, M. & Taylor, G. (1996a). Pressure surge case studies. In: *Proc. of 7th Int. Conf on Pressure Surges and Fluid Transients in Pipelines and Open Channels*, BHR Group, Harrogate, U.K.

Hamilton, M. & Taylor, G. (1996b). Pressure surge criteria for acceptability. In:*Proc. of 7th Int Conf on Pressure Surges and Fluid Transients in Pipelines and Open Channels*, BHR Group, Harrogate, U.K.

Heinsbroek, A. & Tijsseling, A. (1994). The influence of support rigidity on water-hammer pressures and pipe stresses. In: *Proc of 2nd Int Conf on Water Pipeline Systems*, BHR Group.

Larsen, T. (1987). The influence of waves on the hydraulics of sea outfalls. In: *Coastal Engineering* 1986. pp. 2578-2584.

Lavooij, C. & Tijsseling, A. S. (1989). Fluid-Structure Interaction in compliant piping systems. In: *Proc., 6th Int. Conf. on Pressure Surges*, Cambridge, U.K.

Locher, F., Huntamer, J. & O'Sullivan, J. (2000). Caution: pressure surges in process and industrial systems may be fatal. In: *BHR Group Conference Serie*s, vol. 39. Bury St. Edmunds; Professional Engineering Publishing.

Tijsseling, A. & Lavooij, C. (1990). Waterhammer with Fluid-Structure Interaction. *Applied Scientific Research* 47(3), 273-285.

Tijsseling, A. & Vardy, A. (1996). Axial modelling and testing of a pipe rack. In: *BHR group conference series publication*, vol. 19. Mechanical Engineering Publications Limited.

Tijsseling, A. S. (1993). *Fluid-structure interaction in case of water hammer with cavitation*. Ph. D. Thesis.

Weaver Jr, W., Timoshenko, S. P. & Young, D. H. (1990). *Vibration problems in engineering*, ISBN 978-0-471-63228-3. John Wiley & Sons.

Wu, J.-S. & Shih, P.-Y. (2001). The dynamic analysis of a multispan fluid-conveying pipe subjected to external load. Journal of Sound and Vibration 239(2), 201-215.

Yang, K., Li, Q. & Zhang, L. (2004). Longitudinal vibration analysis of multi-span liquid-filled pipelines with rigid constraints. *Journal of Sound and Vibration* 273(1), 125-147.

Zhang, L., Tijsseling, S. & Vardy, E. (1999). FSI analysis of liquid-filled pipes. *Journal of sound and vibration* 224(1), 69-99.

Zhang, X., Huang, S. & Wang, Y. (1994). The FEM of fluid structure interaction in piping pressure transients. In: *Proceedings of the First International Conference on Flow Interaction*, Hong Kong.